ISSN 0040-6015, Thermal Engineering, 2016, Vol. 63, No. 9, pp. 648–656. © Pleiades Publishing, Inc., 2016.
Original Russian Text © V.D. Loktionov, E.S. Mukhtarov, 2016, published in Teploenergetika.

NUCLEAR POWER PLANTS

Estimation of Thermal Loads on the VVER Vessel under Conditions of Inversion of the Stratified Molten Pool in a Severe Accident

V. D. Loktionov* and E. S. Mukhtarov

Moscow Power Engineering Institute, ul. Krasnokazarmennaya 14, Moscow, 111250 Russia

**e-mail: haevec@yandex.ru*

Abstract—Analysis of the thermal state of molten pools that can be formed on the vessel bottom of the VVER-600 medium-power reactor during a severe anticipated accident with melting of the core is represented. Two types of the molten pool of core materials, with the two-layer and inverse three-layer stratification, are considered. Thermal loads acting on the reactor vessel from the melt are estimated depending on its formation time. Features of the thermal state of the melt in the case of its inverse stratification are analyzed. It is shown that thermal loads on the reactor vessel exceed the critical heat flux (CHF) when forming the two-layer stratified molten pool 10 and 24 h after its shutdown, and the thermal load is close to the corresponding CHF or somewhat exceeds it in 72 h. In the case of the formation of the inverse structure of the melt, one can observe a decrease by more than 2.5 times (in comparison with the two-layer stratified structure) in the thermal load on the reactor vessel in the region of its contact with the upper layer of the steel melt. Analysis of results showed that maximum densities of heat flux to the reactor vessel from the bottom metallic layer with the melt inversion did not exceed corresponding CHFs 24 and 72 h after the reactor shutdown. Because the thermal load on the reactor vessel can be localized in the region of its bottom, where the CHF is relatively small, during the inverse stratification of the melt, there is a need to carry out further in-depth experimental and analytical investigations of conditions for formation of the stratified molten pool and to obtain corrected experimental CHFs for conditions and outlines of cooling the external surface of the VVER-600 vessel in a severe accident.

Keywords: severe accident, reactor, VVER, melt, natural convection, temperature, reactor vessel, simulation, stratification, melt inversion, heat generation

DOI: 10.1134/S0040601516090032

Analysis of the possibility for in-vessel retention of the core material melt during the severe anticipated accident (SA) for vessel-type reactors (VVER, PWR, BWR) is based on the knowledge of the thermal state of the vessel structure of the reactor plant (RP), which is subjected to heat action of the high-temperature melt forming in the bottom part of the vessel with the accident development. The reactor heating results in melting of its wall fusion and deformation, because of the high-temperature creep of vessel steel, which finally can result in the damage of the vessel structure and the radioactive material yield beyond it. The possibility for retention of the reactor vessel loading capacity in the SA depends on values and the character of the thermal load distribution over the inner surface of the vessel wall, cooling conditions, and conditions of the force loading of the vessel during the accident [1–9]. As a rule, the analysis of thermal loads on the reactor vessel from the molten pool in the SA is carried out with the supposition that the melt has the two-layer stratified structure [2–8]: the metallic melted layer (steel, zirconium, etc.) is placed over the heat-generation oxide fraction of the melt (Fig. 1a). However, experimental and calculation data [10–16] obtained in recent years show that SA conditions accompanied by the core melting can result in the formation of the melt in the bottom vessel part with the more complex structure of materials of the core and vessel internals (VIs). Pool dimensions and the structure of the melt more substantially affect the thermal load distribution over the reactor vessel and, consequently, its deformation behavior during the accident situation. At the present time, based on experimental data obtained in the context of a number of research programs, for example, MASCA (OECD/NEA), METCOR, and CORPHAD (International Science and Technology Center (ISTC)) [10, 11, 17], one can suppose that the certain stage of the SA development in vessel reactors can form the molten pool with the inverse stratified structure. In this case, the possibility is for the displacement of more dense metallic components (uranium and its compounds with iron, nickel, chromium, and zirconium) into the bottom part of the melt because of the uranium and zirconium extraction from the oxide fraction of the melt (Fig. 1b). Because such metallic melt phase has the residual heat genera-

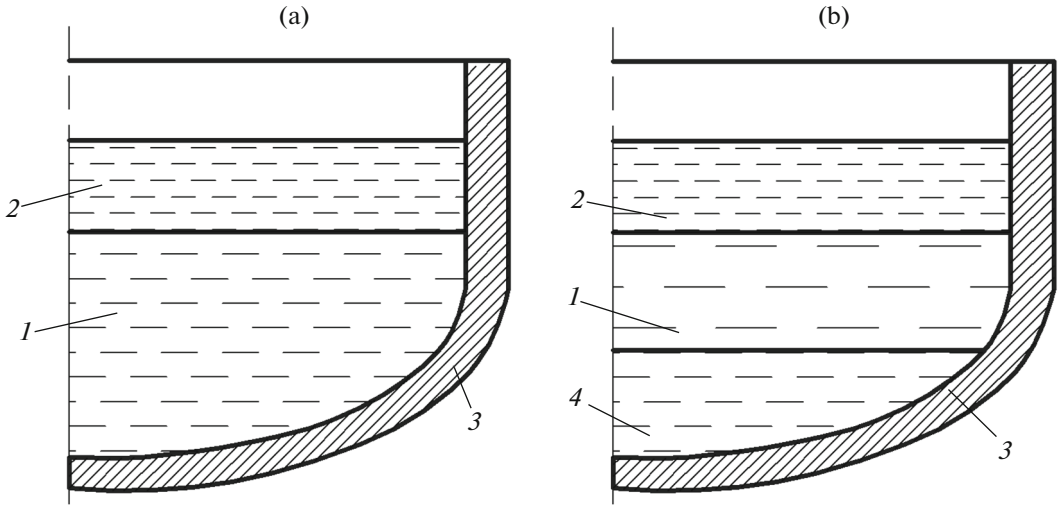

Fig. 1. Structure of (a) two-layer and (b) inverse three-layer molten pools in the VVER vessel. (*1*) oxide melt, (*2*) upper metallic layer, (*3*) reactor vessel, and (*4*) bottom metallic layer.

tion and the high heat conduction (in comparison with the oxide fraction of the melt), one can expect the substantial redistribution of the thermal load on the reactor vessel wall in comparison with the traditional two-layer melt structure. In spite of the absence of complete data at present on conditions of formation of the inverse stratified melt in the SA, there is the objective necessity to study features of the melt behavior with such structure and its effect on the thermal state of the reactor vessel structure under conditions of the SA [12–15]. The necessity and actuality of similar investigations as applied to the RP of VVER are determined by the practical absence of data, which allowed us to estimate the effect of the formation of the dense metallic phase in the bottom part of the molten pool on the thermal state of the reactor vessel structure.

RESEARCH OBJECTIVES AND INITIAL DATA

The general objectives of the research are the estimation of thermal loads that act on the reactor vessel from the molten pool and the study of features of the behavior of the inverse stratified melt, which can form in the bottom part of the reactor vessel during the anticipated SA. The thermal analysis of the molten pool was carried out for the VVER-600 medium-power reactor based on the numerical simulation of thermohydrodynamic processes in the melt subject to natural convection and thermal effects of melting/solidification. For purposes of the study of the influence of the melt structure on the thermal load and the character of its distribution over the reactor vessel surface, parametric numerical computations were carried out for two scenarios of the SA: the formation of the two-layer molten pool in one (metallic layer of the melt is over its oxide heat-generating part) and the pool of the inverse three-layer stratified melt forms in the other (metallic melt layers are above and lower than the oxide layer). Numerical simulation for both scenarios was carried out for different times from the time of the reactor shutdown (initial event) that allowed us to estimate a change in the thermal load to the reactor vessel depending on the residual heat generation in the melt:

Time after initial event, τ, h	10	24	72	120
Power of residual heat generation in melt W_{res}, MW	11.6	9.6	6.7	5.5

The power of the residual heat generation in the melt was accepted according to ISO 10645:92 Standard, based on the nominal thermal power of VVER-600, which was approximately 1600 MW, without the consideration of a decrease in the power of the residual heat generation in the melt as a result of the volatile fission-product yield.

In the simulation of the melt behavior in various time stations, we assumed that the melt incoming the lower chamber of the reactor vessel occurs instantly (so-called “volley” inflow). It should be noted that times equal to 24 and 72 h correspond to the termination time of the operation of passive safety systems and are taken conservatively according to [9] as two basic computational events of the SA for the RP with the reactor of the given type.

The composition of the melt incoming the vessel bottom during the accident depends on many conditions and factors characterizing the SA occurring mode (degree of core damage, degree of zirconium oxidation, etc.). In view of the significant uncertainty in the estimation of the quality and dynamics of incoming of core materials in the bottom part of the

Composition of the melt formed in a bottom part of the reactor vessel in the SA

Corium component	Component weight, t				
	two-layer stratified melt [16]		three-layer melt with inverse stratification		
	metallic layer (top)	oxide layer (bottom)	metallic layer (top)	oxide layer (middle)	metallic layer (bottom)
Steel (iron, nickel, chromium, etc.)	31.0	–	25.0	–	17.4
Zirconium	6.2	–	8.0	–	3.1
Uranium dioxide	–	64.0	–	51.5	–
Zirconium dioxide	–	16.5	–	11.7	–
Uranium extracted	–	–	–	–	10.6
Weight (in layers), t	37.2	80.5	33.0	63.2	31.1
Total weight, t	117.7		127.3		

reactor in the SA, we took data [16] listed in the table as a base.

In the determination of the final composition of the three-layer corium after attainment by it of the conditionally equilibrium state (see table), we considered extraction of metallic uranium and zirconium from the oxide fraction of the melt, initial degree of zirconium oxidation, and initial weight of steel involved into extraction of uranium and zirconium from the oxide fraction of the melt. The amount of components both for the oxide and for bottom metallic phase of the melt was determined in accordance with experimental and computed data [10–17].

When finding weights of extracted uranium and zirconium involved in the formation of the bottom metallic melt layer, we supposed that the initial degree of zirconium oxidation and the initial composition of the melt were the following: initial degree of zirconium oxidation is 0.3; initial steel weight, 20 t; uranium dioxide weight, 64 t; and zirconium weight, 16 t.

For two variants of the inverse stratification of the melt, we assumed that the upper metallic melt layer formed after the formation of the bottom metallic and oxide layers of the melt and the termination of uranium and zirconium extraction as a result of incoming of additional melted materials (steel and zirconium) from the upper part of the core and VIs. By data [11, 12, 16–18], the formation of the inverse structure of the molten pool is possible at the degree of an initial zirconium oxidation of approximately 0.2–0.4, ratio of approximately 0.3 for the steel weight to the oxide fraction of the melt, and uranium–zirconium ratio of approximately 1.0–1.3 for the reactor structure. Since the uranium–zirconium ratio is close to 1.2 for the VVER-600 structure [16], the possibility for the formation of the inverse melt structure as one of its probable transient state is completely substantiated. Because metallic uranium displaces in the bottom metallic melt layer during extraction, this layer has inherent heat generation. When determining residual heat, which is distributed between the oxide phase and the bottom metallic melt layer during extraction, it was accepted that all initial residual heat generation in the oxide molten pool was provided by UO_2, and uranium during extraction from the oxide phase (UO_2) transferred in the bottom metallic melt layer, having the residual heat generation corresponding to the amount of UO_2, from which it was extracted.

Thus, taking into account the corium composition with the inverse melt structure (see table), we can determine that the residual heat generation in the molten pool is distributed between the oxide and bottom metallic layer in a percentage ratio as 80 : 20, respectively. To estimate the effect of the uncertainty caused by a difference in scenarios of occurrence of the SA upon the behavior of the inverse melt, computations were carried out also for another ratio of the residual heat generation between its oxide and bottom metallic layers.

When carrying out numerical simulation of the thermal state of the melt, it is supposed that the simulation region is bounded by the molten pool with taking corresponding boundary conditions [4, 6, 7, 19, 20]. The thermal state of the reactor vessel was not considered in the given analysis. Characteristic dimensions of the molten pool corresponded to inner dimensions of the VVER-600 vessel [16].

COMPUTATION PROCEDURE AND GENERAL ASSUMPTIONS

Analysis of the thermal state of the two-layer molten pool composed of the layer of heat-generation components of the corium with thickness h and the metallic layer (mainly of steel) with thickness h_{st} (Fig. 2) was realized subject to natural convection in the melt. The configuration and dimensions of the molten pool correspond to the shape and inner dimensions of the vessel bottom of the reactor of the type considered [16]. Because the melting temperature of the reactor vessel material is lower than the solidus temperature of the corium, a corium crust (skull)

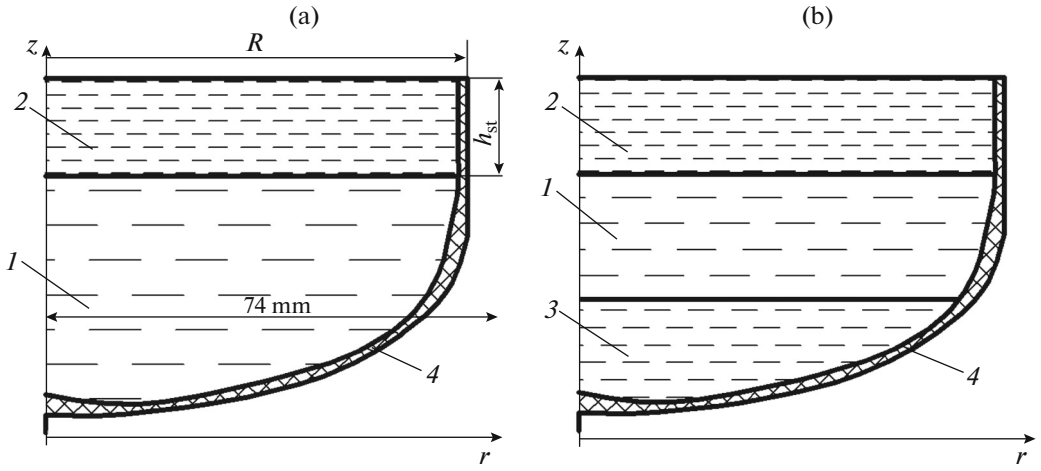

Fig. 2. Analytical model of the problem for (a) two-layer and (b) inverse molten pools. $R = 1.91$ m is the pool radius; (*1*) oxide melt, (*2*) upper metallic layer, (*3*) bottom metallic layer, and (*4*) corium.

forms on the inner surface of the vessel wall (in the region of the contact with the melt). Therefore, to simplify the simulation of thermohydrodynamic processes in the corium, the computation region can be bounded by the molten pool (Fig. 2), giving the corresponding boundary conditions at the corium–reactor vessel interface. For example, in the case of the two-layer molten pool (Fig. 2a), the temperature at the interface of the vessel–oxide layer of the melt was taken to be equal to the melting temperature of the corium (approximately 2700 K), while that at the contact with the metallic layer was taken to be equal to the melting temperature of steel (approximately 1800 K). For the inverse melt structure (Fig. 2b), it was additionally accepted that the temperature at the contact of the vessel and the bottom metallic layer is 2600 K. Heat fluxes to the reactor vessel from the heat-generating corium were determined subject to the conjugacy of thermal processes in the metallic and oxide phases of the melt. Numerical simulation of these processes was carried out using the computing method for free-convective heat-and-mass transfer in the heat-generating liquid at the high Relay numbers [6, 19–21], i.e., on the dominance of the thermogravitational mechanism of the turbulence initiation.

When solving the problem considered, we used the mathematical model in which the turbulent convection in the liquid phase was considered by means of using the effective heat conduction and diffusion coefficients, including the molecular and turbulent components [21], which allows us to refuse to solve motion equation. At the same time, equations of heat conduction and diffusion of melt components are solved by the shock-capturing method in the whole computed region in which are metallic melt layer and the oxide corium. The given mathematical model is successfully realized in the context of the NARAL/FEM two-dimension finite-element computer code [4, 6, 7, 19, 20], whose verification was fulfilled on a wide range of test problems of heat conduction and convection at the high and low Relay numbers and different dimensions of the computed region. Results of fulfilled test computations well agree both with experimental and with computed data of other authors.

Numerical simulation was carried out with the following assumptions:

(1) heat-generating phase of the molten pool presents the homogeneous system of oxides UO_2 and ZrO_2, computations use its effective thermophysical parameters;

(2) melting/solidification process in the melt is simulated as melting in the pure substance;

(3) forming skull "closely covers" (ideal thermal contact) the inner surface of the reactor vessel wall; and

(4) melting of the reactor vessel wall has no effect on the shape and dimensions of the molten pool.

ANALYSIS OF NUMERICAL SIMULATION RESULTS

Figures from 3 to 8 represent results of numerical simulation of the thermal state of the two-layer (Figs. 3, 4, and 5) and inverse three-layer (Figs. 6, 7, and 8) molten pools for different time slices after the initial event. Comparison of Figs. 3a and 3b showed that there is a similarity of the thermal state of the melt in 24–72 h after the reactor shutdown. The temperature stratification of the corium occurs in the bottom (oxide) melt fraction, and the maximum temperature of the upper (metallic) melt layer is observed in its center. The difference between maximum temperatures in this layer is approximately 100 K in instant times considered.

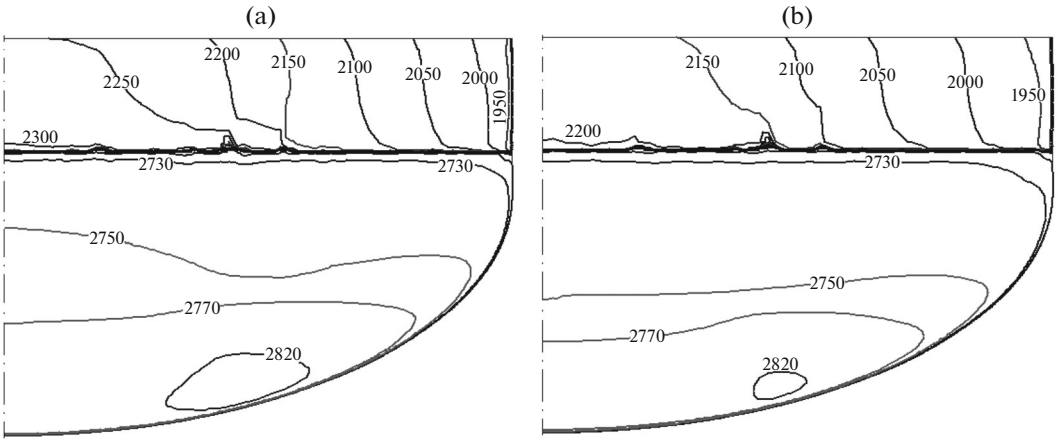

Fig. 3. Thermal state of the two-layer molten pool at its formation time of (a) 24 h and (b) 72 h after the initial event. W_{res}, MW: (a) 9.6, (b) 6.7.

To estimate the possibility for the in-vessel retention of the melt during the SA, there is a need to know the distribution of the heat flux density over the side surface of the molten pool. Figure 4a illustrates the profile of the distribution of thermal load q_{side} over reactor vessel generatrix S in the region of its contact with the molten pool, and Fig. 4b illustrates that of q_{upp} over radius r of the upper surface of the steel melt layer.

In the case of the SA, one of general criteria of the integrity protection of the reactor vessel structure is the absence of through fusion of the vessel wall during the accident, which is provided if the thermal load on the reactor vessel wall does not exceed the CHF q_{cr} at the external surface of the vessel wall surface. Therefore, computed values of the density of heat flux at the molten pool boundary were compared with CHFs being the reliable experimental data that were obtained in experiments on heated models having the shape and bottom dimensions that corresponds to geometric parameters of reactor vessel [22]. Based on a restricted number of experimental data on conditions of the external cooling of the vessel, we took the following formulas for estimation of the CHF, which were obtained on large-scale models of the VVER vessel in the absence of the director case [23]:

$$q_{cr}(\varphi) = 300 + 12.8\varphi \text{ at } 0 < \varphi < 32°; \quad (1)$$

$$q_{cr}(\varphi) = 710 + 2.85(\varphi - 32°) \text{ at } 32 < \varphi < 90°, \quad (2)$$

where q_{cr} is expressed in kilowatt per square meter; and φ is the slope angle of the generatrix of the external surface of the vessel, rad;

and for case of the outer cooling of the vessel with the nucleate boiling of water in the large volume [16]:

$$q_{cr}(\varphi) = (1 + 0.036\Delta T_{sub}) \times (0.434 + 0.347\varphi + 0.0604\varphi^2), \quad (3)$$

where q_{cr} is expressed in megawatt per square meter; ΔT_{sub} is water subcooling to the vapor saturation temperature, accepting $\Delta T_{sub} = 1$ K.

As is evident from graphs in Fig. 4, at times of the molten pool formation that is 10 and 24 h, the heat flux density to the reactor vessel in the region of its contact with the steel melt layer (layer boundaries in Fig. 4 are designated as *RPV Wall*) significantly exceeds corresponding CHFs. At a time of 72 h for the molten pool formation, the maximum heat flux density was 1150 kW/m^2, which exceeds CHFs determined by (1) and (2), and is compared with the CHF computed by (3). Taking into account that formula (3) was obtained for foreign reactors, as a rule, with the semispherical bottom of the vessel, the use of this relationship for determination of the CHF in domestic VVERs can be only under the condition of the comprehensive and substantiated verification of its availability.

The heat flux density in the contact region of the oxide layer with the reactor vessel was found to be significantly lower than the CHF that well agrees with previously obtained results [9, 16].

The heat flux density at the upper steel melt surface (Fig. 4b) is substantially lower than the thermal load on the side surface of this melt layer and does not exceed 220 kW/m^2 (at a molten pool formation time of 10 h). The thermal load on the melt surface conditions both the heating intensity on the reactor vessel wall placed above the molten pool and dynamics of core heating and melting.

The residual heat generation power decreases with time after the initial event. The maximum heat flux density correspondingly changes approximately from 2000 to 850 kW/m^2 ($q_{side\ max}$) to the reactor vessel in the region of its contact with the molten pool and from 200 to 150 kW/m^2 ($q_{upp\ max}$) at the upper surface of the steel melt layer in 10–120 h (Fig. 5).

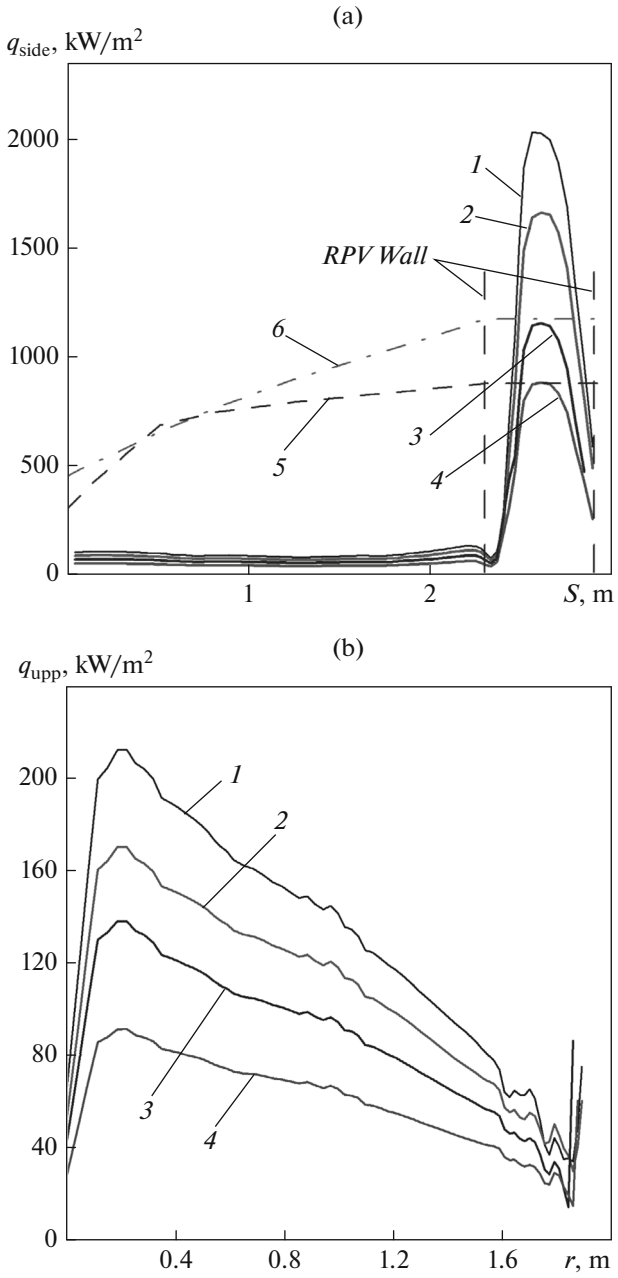

Fig. 4. Heat flux density distribution (a) over the generatrix of the side surface of the reactor vessel and (b) along the upper surface radius of the two-layer molten pool. τ, h: (*1*) 10, (*2*) 24, (*3*) 72, and (*4*) 120; changing the CHF: (*5*) by (1) and (2) and (*6*) by (3).

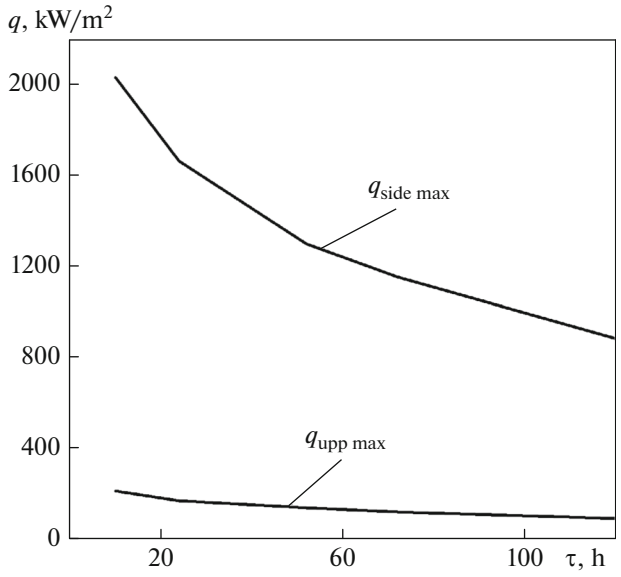

Fig. 5. Maximum heat flux density at the side and upper surfaces of the metallic melt layer as a function of the time of the two-layer molten pool formation after the initialevent.

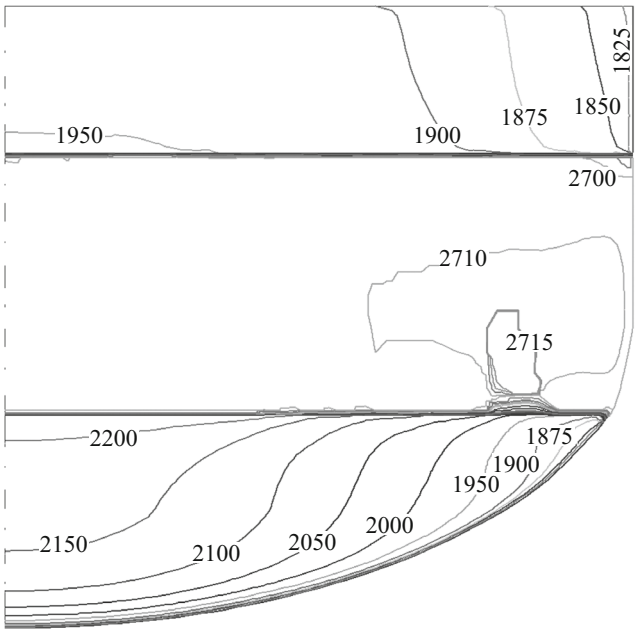

Fig. 6. Thermal state of the three-layer inverse stratified molten pool 72 h after the initial event.

Of special interest is analysis of the thermal state of the melt and the thermal load on the reactor vessel during the formation of the three-layer inverse molten pool. Simulation of the thermal state of such melt was carried out for two scenarios of the accident. In the basic scenario, the corium composition was represented by data of the table, which corresponded to the distribution of the residual heat between the oxide phase and the bottom metallic melt layer in a percentage ratio of 80 : 20 (Figs. 6 and 7). The ratio of the weight of metallic extracted uranium to the total weight of the bottom metallic melt layer is less than 0.3. At the same time, according to research results [11], the formation of compositions of metallic uranium and iron with a uranium content of no less than 70% is possible. The question on the probability of the appearance of similar compositions and the formation of the bottom metallic layer of the molten pool from them during the

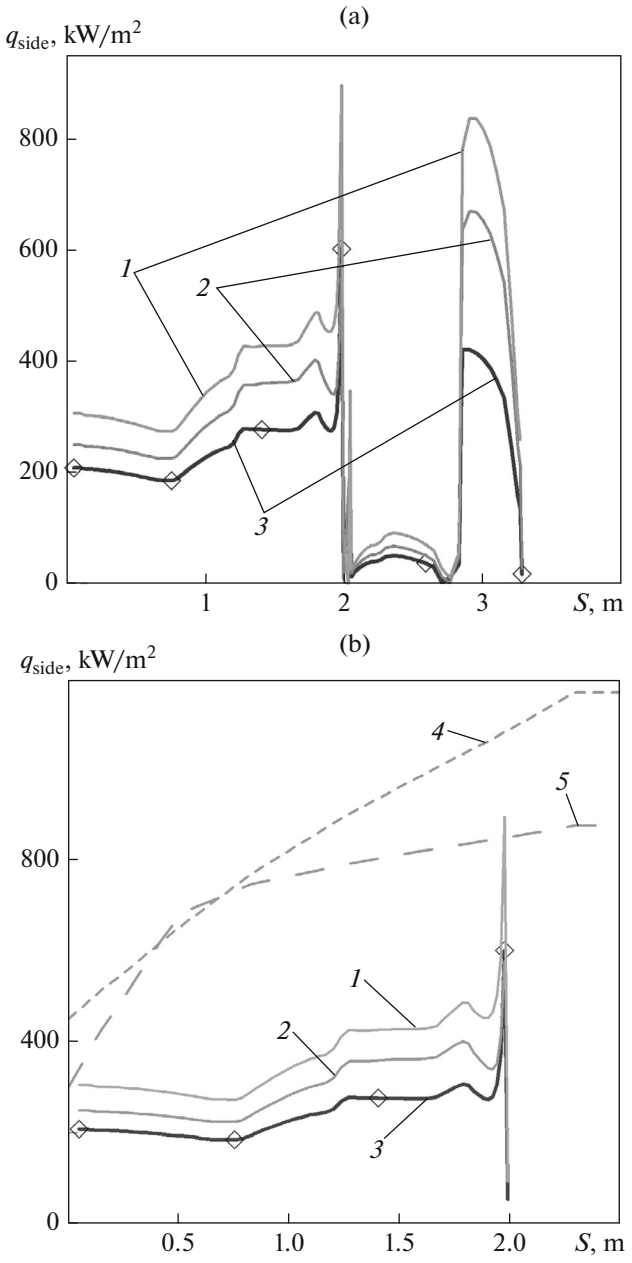

Fig. 7. Heat flux density distribution over the generatrix of the inner surface of the reactor vessel wall at different times of the formation of (a) the three-layer molten pool and (b) its bottom metallic layer. τ, h: (*1*) 10, (*2*) 24, (*3*) 72; changing the CHF: (*4*) by (3) and (*5*) by (1) and (2**).**

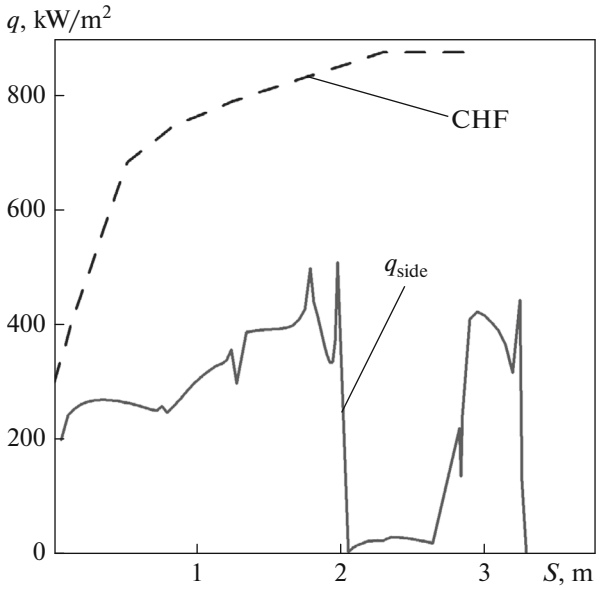

Fig. 8. Heat flux density distribution over the generatrix of the inner surface of the reactor vessel wall for the inverse three-layer molten pool and changing the CHF over the external surface of the vessel according to (1) and (2) 72 h after the initial event.

SA remains open up to now, and to solve it finally there is a need to carry out further profound experimental and computational investigations and additional study of determining thermophysical processes in similar scenarios of the SA. Because of such uncertainty, we decided also to consider the accident scenario at which the bottom metallic melt layer gets the greater amount of extracted metallic uranium than in the above-considered variant with the distribution of residual heat between the oxide phase and the bottom metallic layer in a percentage ratio of 55 : 45 (Fig. 8).

Figure 6 represents the thermal state of the molten pool 72 h after the initial event in VVER-600 with the residual heat distribution between phases in a percentage ratio of 80 : 20. Comparison of the variant considered with the similar one (pool formation time of 72 h) for the two-layer molten pool (Fig. 3b) showed a substantial decrease in the temperature (more than by 250 K) and the heat flux density (more than by 2.5 times) at the side surface of the upper steel melt layer (Fig. 7a). As a result, the thermal load that acts on the vessel wall in the region of its contact with the upper metallic layer was found to be lower than corresponding CHFs determined by (1)–(3) at molten pool formation times of 24 and 72 h (Fig. 7a). As is evident, the formation of the inverse melt structure in comparison with the two-layer molten pool (Fig. 4) resulted in a significant (approximately by 2.5 times) decrease in the heat load acted on the reactor vessel in the region of its contact with the upper metallic melt layer at the same total power of residual heat generation. It should be added that dimensions (aspect ratio) of the upper metallic melt layer in two variants considered were taken as practically equal in order that the comparison of simulation results was rightful.

Analysis of the thermal state of the bottom metallic melt layer after inversion shows that its temperature stratification is observed in the quasistationary state of the melt, and the region with the highest temperature is in the central part of the layer under the upper oxide

heat-generation layer of the corium (Fig. 6). The maximum temperature in the bottom metallic layer considered attains 2200 K, which is significantly lower (more than by 600 K) than at the two-layer stratification (Fig. 3b). This is explained by the fact that the bottom metallic melt layer having inherent heat generation has the higher coefficient of heat transfer to the reactor vessel surface in comparison with the oxide phase of the melt. This is verified by the analysis of the heat flux density distribution on the side surface of the bottom metallic melt layer (Fig. 7b), from which it follows that the heat flux density in the bottom region of the three-layer molten pool is substantially higher than under the same conditions with the two-layer stratification. At the same time, maximum thermal loads are observed in the near-boundary region of the contact of the oxide phase and the bottom metallic melt layer, and the heat flux density in this region exceeds similar values for the upper metallic melt layer (Fig. 7), but does not exceed corresponding CHFs at melt formation times of 24 and 72 h (Fig. 7b).

When the residual heat generation is redistributed between the oxide and bottom metallic melt layer as 55 : 45 in the percentage ratio, the thermal load on the vessel bottom is somewhat higher (Fig. 8) than in the considered basic scenario (Fig. 7). With allowance made for the fact that CHFs have relatively small values in the region of the VVER bottom, where thermal loads act from the bottom metallic melt layer, problems of the realization of the stable and effective heat removal from the external surface of the reactor vessel in this region become very urgent for provision of the in-vessel retention of the melt in the case of the SA.

CONCLUSIONS

(1) When forming the two-layer stratified molten pool 10 and 24 h after the initial event, thermal loads exceed corresponding CHFs. In 72 h, the thermal load is close to corresponding CHFs or somewhat exceeds them. Because conservative assumptions were made in computations in the present research, there is a need to carry out additional in-depth studies of the thermal state of the molten pool for different scenario of its formation in the SA. This makes it possible to more correctly and reasonably determine regions and conditions of crisis-free cooling of the VVER-600 vessel in the SA.

(2) In the case of the formation of the inverse melt structure, there is a decrease in the temperature (more than by 250 K) and the heat flux density (more than by 2.5 times) at the contact of the reactor vessel and the side surface of the upper metallic layer, and the thermal load on the reactor vessel bottom increases.

(3) The heat flux density at the side surface of the molten pool in the region of the bottom metallic layer was found to be substantially higher with the inverse stratification of the corium than with the two-layer stratification. The thermal load in the region of the bottom metallic layer does not exceed corresponding CHFs at a molten pool formation time of 24 and 72 h after the initial event.

(4) In-depth experimental and analytical studies are required with the following purposes:

(a) study of conditions for formation of the inverse stratified molten pool in the SA;

(b) determination of the residual heat generation distribution between melt phases with its inverse stratification; and

(c) obtaining of improved CHFs that most completely correspond to the actual flow diagram of cooling of the external surface of the VVER-600 vessel in the SA.

REFERENCES

1. V. V. Pazhetnov, V. P. Semishkin, A. N. Churkin, V. D. Loktionov, K. S. Dolganov, D. Yu. Tomaschik, A. S. Filippov, N. I. Drobyshevsky, and A. M. Danilov, "Consideration of conditions of prolonged exposure of the molten core fragments to WWPR-440 reactor pressure vessel during severe accidents," Vopr. At. Nauki Tekhn., Ser. Obespech.Bezop. AES, No. 25, 161–172 (2009).
2. V. D. Loktionov, "Parametric analysis of the failure of a WWPR-440 vessel during a serious accident," At. Energy **103**, 986–989 (2007).
3. V. D. Loktionov, V. P. Semishkin, V. V. Pazhetnov, and V. A. Mokhov, "Study of WWPR vessel behavior for justification of the possibility of intervessel keeping of smelt at severe accident," Vopr. At. Nauki Tekhn., Ser. Obespech. Bezopasn. AES, No. 15, 65–72 (2006).
4. N. G. Rassokhin, V. D. Loktionov, and E. S. Mukhtarov, "A combined thermal and strength analysis of the behavior of a WWPR-440 reactor's vessel during an accident involving core melting," Therm. Eng. **53**, 675–681 (2006).
5. V. D. Loktionov, "Estimation of conditions and destruction time for WWPR-440 reactor vessel under the case of severe accident with core melting," Vestn. Mos. Energ. Inst., No. 5, 43–48 (2006).
6. N. G. Rassokhin, V. D. Loktionov, E. S. Mukhtarov, V. E. Orlov, and K. E. Molodyk, "Numerical simulation of heat transfer when retaining the core melt in the reactor vessel," Therm. Eng. **45**, 495–504 (1998).
7. E. S. Loktionov, N. I. Mukhtarov, V. E. Yaroshenko, and V. E. Orlov, "Numerical investigation of the reactor pressure vessel behavior under severe accident conditions taking into account of the associated processes of the vessel creep phenomenon and the molten pool natural convection," Nucl. Eng. Design **191**, 31–52 (1998).
8. M. F. Rogov, S. A. Logvinov, V. S. Granovskii, S. V. Kovtunova, V. B. Khabenskii, V. V. Bezlepkin, and I. V. Kukhtevich, "Analyzing the possibility of retaining the corium in the vessel of a WWPR-640 reactor in a severe accident with a damaged core," Therm. Eng. **43**, 888–892 (1996).

9. S. I. Pantyushin, A. I. Frizen, S. I. Asadskii, V. P. Semishkin, D. O. Veselov, N. V. Bukin, M. A. Bykov, V. A. Mokhov, A. L. Volchek, Yu. A. Zvonarev, V. F. Strizhov, A. E. Kiselev, A. S. Filippov, N. I. Drobyshevskii, K. S. Dolganov, and E. V. Moiseenko, "Development of system of smelt keeping and reactor vessel cooling at severe beyond design basis accidents for atomic power stations with RU WWPR-600 and RU WWPR TOI, Vopr. At. Nauki Tekhn. Ser. Obesp. Bezop. AES, No. **30**, 45–59 (2011).
10. V. G. Asmolov, V. N. Zagryazkin, D. F. Tsurikov, Yu. G. Degal'tsev, V. Yu. Vishnevskii, E. K. D'yakov, A. Yu. Kotov, and V. M. Repnikov, "Investigation of the interaction of oxide melt and steel in a WWPR-1000 vessel during a serious accident," At. Energy **104**, 273–277 (2008).
11. V. S. Bechta, V. B. Granovsky, V. V. Khabensky, V. I. Gusarov, L. P. Almiashev, E. V. Mezentseva, S. Yu. Krushinov, R. A. Kotova, M. Kosarevsky, D. Barrachin, F. Bottomley, F. Fichot, and M. Fischer, "Corium phase equilibria based on MASCA, METCOR and CORPHAD results," Nucl. Eng. Des. **238**, 2761–2771 (2008).
12. A. Nieminen, The effect of late-phase melt pool configuration on pressure vessel rupture, *Proc. 6th Europ. Rev. Meeting on Severe Accident Res. (ERMSAR-2013)*. Avignon (France), 2013, pp. 1–16.
13. M. Fukasawa, S. Hayakawa, and M. Saito, "Thermal-hydraulic analysis for inversely stratified molten corium in lower vessel," J. Nucl. Sci. Technol. **45**, 873–888 (2008).
14. M. Fukasawa and S. Tamura, "Thermodynamic analysis for molten corium stratification test MASCA with ionic liquid U–Zr–Fe–O–B–C–FPs database," J. Nucl. Sci. Technol. **44**, 1210–1219 (2007).
15. K. H. Kang, "Experimental and analytical investigation on the layer inversion of melt pool during the severe accidents in the APR1400," *Proc. 8th Int. Topical Meeting on Nuclear Thermal-Hydraulics, Operation and Safety,* China, Shanghai, 2010.
16. Yu. A. Zvonarev, M. A. Budaev, A. M. Volchek, V. A. Gorbaev, V. N. Zagryazkin, N. P. Kiselev, V. L. Kobzar', A. V. Konobeev, and D. F. Tsurikov, "Calculation analysis of melt active zone keeping in reactor vessel at severe accidents on atomic power stations with WWPR," *Proc. 7th Int. Sci.-Tech. Conf. "Ensuring of Safety of Atomic Power Stations with WWPR"* (Podol'sk, Russia, 2011).
17. D. F. Tsurikov, V. N. Zagryazkin, V. Yu. Vishnevskii, E. K. D'yakov, A. Yu. Kotov, and V. M. Repnikov, "U–Zr–Fe–O melt density," At. Energy **107**, 247–254 (2009).
18. V. G. Asmolov, V. N. Zagryazkin, and D. F. Tsurikov, "The thermodynamics of U–Zr–Fe–O melts," High Temper. **45**, 305–312 (2007).
19. L. A. Dombrovskii, L. I. Zaichik, Yu. A. Zeigarnik, E. S. Mukhtarov, and A. S. Sidorov, "Calculations of heat flowrates to the WWPR-440 reactor vessel during interaction of corium melt with the reactor vessel," Therm. Eng. **53**, 303–306 (2006).
20. L. A. Dombrovskii, L. I. Zaichik, Yu. A. Zeigarnik, E. S. Mukhtarov, and A. S. Sidorov, "Development of the corium bath during the melting of a WWPR-440 reactor core," Therm. Eng. **52**, 396–402 (2005).
21. L. A. Dombrovskii, L. I. Zaichik, and Yu. A. Zeigarnik, "A model of effective heat conduction for calculating free-convection heat exchange at large Rayleigh numbers," Dokl. Phys. **44** (6), 358–361 (1999).
22. V. D. Loktionov, V. V. Pazhetnov, and G. G. Yan'kov, "Eksperimental-calculation studies of WWPR vessel cooling at severe accident in the conditions of high thermal loadings," *Proc. 8th Int. Sci.-Tech. Conf. "Ensuring of Safety of Atomic Power Stations with WWPR"* (Podol'sk, Russia, 2013).
23. S. A. Logvinov, Yu. A. Bezrukov, and Yu. G. Dragunov, *Experimental Foundation of Thermalhydraulic Safety of WWPR Reactors*, (IzDAT, Moscow, 2003) [in Russian], pp. 84–90.

Translated by S. Ordzhonikidze